Sediment transport and shoreline erosion induced by bichromatic waves with varying group period

J.M. Alsina
Department of Civil and Environmental Engineering, Imperial College London, The United Kingdom

J. van der Zanden & J.S. Ribberink
Marine and Fluvial Systems Group, University of Twente, Enschede, The Netherlands

I. Cáceres
Laboratori d'Enginyeria Marítima, Universitat Politécnica de Catalunya, Barcelona, Spain

ABSTRACT: In the present paper, large scale experimental data are presented showing sediment transport and beach profile evolution at the inner surf zone, close to the shoreline. Four different bichromatic wave conditions have been generated characterized by a similar energy content but varying the wave group period (frequency bandwidth). The differences in the shoreline evolution and associated sediment transport are explained from the differences in the wave group period. It has been shown that increasing the wave group period promotes a seaward horizontal displacement in the shoreline erosion pattern. The inner surf zone shows larger erosion for increasing wave group periods. However at the swash zone larger wave group periods show a berm located further seaward with a relatively less shoreline retreat. Differences in the beach profile evolution are explained from the bandwidth influence in the propagation of wave groups and associated long wave. Larger wave group periods showed a progressive long wave pattern with the associated long wave out of phase with the wave group envelope. This resulted in negative long-wave induced sediment transport within the inner surf zone. Reduced wave group periods have shown a standing pattern that resulted in long wave motions in and out of phase with the wave group envelope depending on the cross-shore location. Within the inner surf zone this resulted in mostly positive long wave induced sediment transport for reduced wave group periods. It was also shown that the long wave induced sediment transport represented on average 18% of the total mobilized sediment transport.

1 INTRODUCTION

Random short swell waves tend to form wave groups during propagation, arriving to the shoreline with a certain degree of groupiness depending on wave condition. Wave groups are widely recognize to be important in Coastal Engineering. Wave groups affect to the design of coastal structures and the operationality of harbours by inducing agitation and energy at long periods. They are also important in predicting sediment transport and coastal morphology.

High frequency (*hf*) wave groups promote low frequency (*lf*) motions by the local depression in water level that occurs beneath larger waves within a group due to variations in radiation stress (Longuet-Higgins and Stewart, 1962, Longuet-Higgins and Stewart, 1964) or by a varying breakpoint mechanism due to the breakpoint location variability induced by the wave groupiness (Symonds et al., 1982). In shallow waters the low frequency motions growth in amplitude while short swell components dissipate due to wave breaking. Runup saturation has been widely demonstrated for short wave frequencies (sea and swell) but it is still unclear if occurs also at low frequency components. Several authors have suggested that saturation potentially extend to the low frequencies during highly energetic conditions hypothesizing an upper limit of *lf* induced runup (van Dongeren et al., 2007). However other studies suggest a linear runup increase with incident wave height (Ruju et al., 2014).

Studies on the relative importance of long wave motion respect to mean or short wave components in sediment fluxes suggest that, outside the surf zone, in general the mean component and short wave components dominate the net sediment transport (Ruessink et al. 1998). However, the relative influence of *lf* motions increases in the inner surf zone as the short wave component dissipates via wave breaking. This increasing *lf* influence has been observed as the wave height to water depth ratio (H/h) reduces in shallow waters, when the water depth reduces faster than wave height, and the long-wave amplitude relative to the water depth become important (Alsina and Cáceres, 2011). An increasing *lf* influence has been also observed in the surf zone, on top of the bar crest as the mean and short wave component often cancel (Ruessink et al., 1998).

Close to the shoreline, at the inner surf zone, several authors (Beach and Sternberg, 1991, Russell, 1993) have observed seaward sediment transport induced by *lf* waves of a similar magnitude that mean currents. On the other hand, at the swash zones a dominance of *lf* motions in dissipative beaches have been reported while in more reflective beaches a larger dominance of incident broken waves has been observed (Miles et al., 2006). Finally, Cáceres and Alsina (2012) have shown the strong importance of long wave induced backwash in the measured shoreline erosion from large scale experimental conditions.

There are, then, evidences of the importance of *lf* motions in beach profile morphology but there is not yet a clear picture of the nature of this influence in terms of magnitude of sediment transport rates and direction. Coastal profile models based on a dominance of mean return flow and wave asymmetry are able of good predictions of the cross-shore bar migration when properly calibrated while the inner surf zone is not as well predicted (Dubarbier et al., 2015). Similarly, recent morphodynamic models (Roelvink et al., 2009) with a description of the *lf* waves dynamics (although they also include short wave influence and mean return flow) are also able of good predictions of beach profile evolution.

The present paper considers this issue and investigates the influence of the wave groups and associated long waves in the beach profile evolution close to the shoreline. Controlled large-scale experiments have been performed over the same initial beach profile configuration, and simulating different wave grouping conditions. Bichromatic waves have been generated, keeping the energy content constant but varying the wave modulation (group frequency). The mechanism behind the distinct measured profile evolution as a function of the wave group period has been analyzed. The paper is organized as follow, the description of the experimental conditions is presented in section 2, the analysis technique and experimental results are showed in section 3 with a discussion of the *lf* motion and wave group influence in the observed dynamic and beach profile evolution. Finally, the main conclusions are discussed and summarized in section 4.

2 EXPERIMENTAL DESCRIPTION

2.1 *Instrumentation*

The experiments were carried out in the large scale wave flume CIEM at Universitat Politecnica de Catalunya (UPC), Barcelona. This is a wave flume 100 m long, 3 m wide, and 4.5 m deep (Figure 1). The experiments were performed under the HYDRALAB-IV CoSSedM (Coupled High Frequency Measurement of Swash Sediment Transport and Morphodynamic) transnational access.

A beach consisting of commercial well sorted sand (d_{50} = 0.25 mm) with an overall mean beach gradient of approximately 1:15 was installed. The measured sediment settling velocity is w_s = 0.034 m/s. The beach commenced 33.3 m from the wavemaker with the toe of the beach at approximately 42 m seaward of the shoreline at SWL. The working water depth was 2.5 m over the horizontal flume section but it was modified around this depth for some specific wave conditions.

The beach was manually reshaped at the beginning of each generated wave condition consisting of the same 1:15 constant beach slope. However small differences appear in the initial shoreline at the still water level (SWL) and some wave conditions were repeated with different working depths. Therefore, two different cross-shore location reference systems are used in the present study. The first reference system is an absolute cross-shore coordinate (X_a) where the x-coordinates are referenced to an absolute fixed value, X_a = 0, corresponding to the lowest position of the wave paddle (this reference system is used in Figure 1). The second reference system (X) is relative to the shoreline location (x_0) at the SWL and the initial beach profile. The relation between the reference systems is $X = X_a - x_0$. X is positive towards the emerged beach and negative towards the wave paddle.

The range of instrumentation utilized (Figure 1) included wire wave gauges (WG) along the length of the flume, Pore Pressure Transducers (PPT) in the surf zone and acoustic wave gauges (AWG) in the inner surf and swash zone.

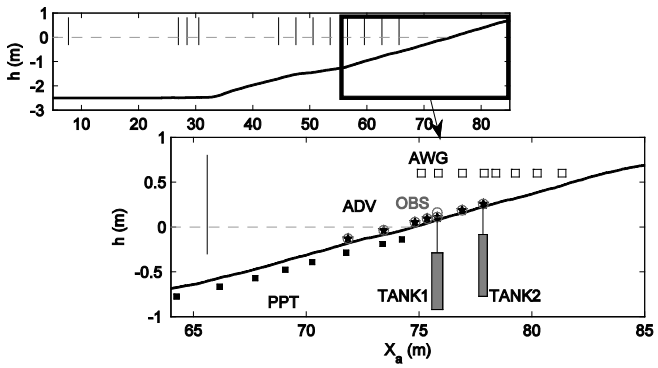

Figure 1. Wave flume layout with instrument locations.

A series of Acoustic Doppler Velocimeters (ADV) and Optical Backscatter Sensors (OBS) were distributed in the surf and swash zones.

The beach evolution along the center-line of the wave flume was measured with a mechanical wheeled bed profiler that measures both the subaerial and submerged beach elevation; more details can be found in Baldock et al. (2011). The vertical coordinate (z) for bed level measurements has the

origin at the still-water level and is negative downward. The overall vertical profile accuracy is estimated to be of ±10 mm.

Two recently developed conductivity based systems, CCM+, (van der Zanden et al., 2015) were installed in the wave flume at two different locations within the swash area, X_a = 75.81 m and 77.8 m respectively for tank 1 and 2. Different tank cross-shore locations within the swash zone were obtained by slightly modifying the working water depth. This is the reason why we have repeated some specific wave conditions with different water depths. This choice was preferred rather than burying the tanks at different locations each time. A more detailed description of the CCM+ system can be found in van der Zanden et al. (2015) with application to one specific wave condition (BE1_2).

2.2 *Wave conditions*

The experimental program was divided into eight different bichromatic wave conditions. The different wave conditions were designed to have the same flux of energy and spectral energy content but different grouping period. The wave conditions measured at a distance of 7.7 m from the toe of the wave paddle are illustrated in Table 1.

The different wave group periods are obtained by maintaining the primary mean frequency f_p constant (keeping the group velocity constant between different wave conditions) but varying f_1 and f_2. The group frequency, f_g is given by $f_g = \Delta f = f_1 - f_2$, and the group period $T_g = 1/f_g$. Broad banded groups (increasing f_1-f_2 difference) lead to shorter groups (reducing T_g) where the energy is distributed in a small number of waves. Narrow banded groups, on the other hand, lead to larger group periods and the same energy is distributed in a larger number of waves per group.

Every wave condition started from the same initial beach profile, consisting on a manually-shaped 1:15 beach profile. For every wave condition, the same wave time series (wave realization or wave test) was repeated eight times (seven for case BE1). Each wave realization has an approximate duration of 30 minutes. The beach profile is measured after every wave realization. The total duration of each wave condition run is of 240 minutes (210 minutes for case BE1) with measurements of 9 profiles (8 plus the initial profile) and the measurement of hydrodynamic variables between measured beach profiles.

Table 1. Generated wave conditions.

Wave Conditions	Component 1		Component 2					
	H_1 (m)	f_1 (Hz)	H_2 (m)	f_2 (Hz)	Δf (Hz)	H/w_sT	Iribarren	d (m)
BE1	0.29	0.303	0.26	0.237	0.0667	3.08	0.40	2.53
BE1_2	0.30	0.303	0.26	0.237	0.0667	3.12	0.40	2.48
BE2	0.26	0.300	0.24	0.240	0.0600	2.81	0.42	2.5
BE3	0.31	0.295	0.31	0.246	0.0500	3.52	0.37	2.5
BE4	0.29	0.288	0.27	0.252	0.0361	3.13	0.40	2.5
BE4_2	0.28	0.288	0.30	0.252	0.0361	3.27	0.39	2.46

3 RESULTS

3.1 *Shoreline erosion and beach profile evolution*

Because all the generated wave conditions had the same energy content and flux of energy. Any differences in shoreline erosion and profile evolution between tests should be attributed to the existing differences in the wave group period (bichromatic bandwith).

Figure 2 shows the final beach profile evolution at the inner surf and swash zones after 210 minutes of experimentation time. It is shown in figure, shoreline erosion resultant of a seaward sediment transport at the inner surf zone and deposition further seaward. The overall beach profile resulted in the formation of a breaker bar (Alsina et al., submitted). Larger shoreline retreat is observed for broad band bichromatic conditions (reduced wave group periods) compared to narrow band conditions.

Berm formation is also observed at locations further onshoreward for increasing bandwith condition. It seems that the influence of decreasing the bichromatic bandwith (increasing the wave group period) is observed in a seaward displacement of the erosion pattern with berm formation further seaward and displacement of the maximum erosion location further seaward. It is indeed noticeable that from x=-2 to x =-4 (inner surf zone), the bed eroded is larger for larger wave group periods (BE3 and BE4 with respect to BE1 and BE2).

3.2 *Wave height at different frequency components*

Wave heights are obtained directly from spectral analysis. Therefore, H_1, H_2 and H_g are obtained as the wave height associated with frequency components 1, 2 and the group frequency. The primary wave height, H is also defined associated with the incident high frequency components 1 and 2.

The cross-shore distribution of the wave height at the short wave components f_1 and f_2 for case BE1 and BE4 representing the limits of smaller and larger wave group periods are showed in Figure 3. Wave heights are averaged using the first 7 measured hydrodynamics runs. Wave breaking locations obtained from the peaks of H/h ratio are also illustrated in Figure 3 with vertical dashed lines. Where H is the short wave height and h is the water depth including measured setup and setdown.

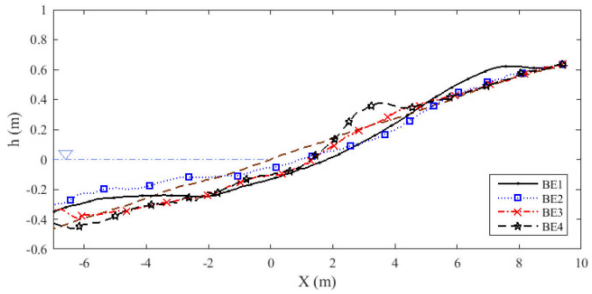

Figure 2. Mean initial beach profile (dash line) and profile evolution for the different wave conditions after 210 minutes of wave action.

The wave height associated with the group frequency (f_g) is also displayed in Figures 3.

It is illustrated in Figure 3 a standing long wave pattern for the wave group component in condition BE1 which is not observed at BE4. BE4 is better characterized by a progressive long wave pattern with long wave height reduction after wave group breaking.

This is better illustrated in figure 4 where phase lag ψ of the low frequency surface elevation with the high frequency wave group envelope and the phase lag ψ of the low frequency surface elevation at consecutive cross-shore locations. Two nodal locations are observed for case BE1 at $X \approx$ -20 m and $X \approx$ -3 m and an antinode at $X \approx$ -10 m. In contrast, wave condition BE4 shows virtually no cross-shore nodal structure at the group frequency. The long wave in BE4 is out of phase with the wave group envelope in the shoaling region (Figure 4b) up to the breaking point.

From this location to the shoreline the phase lag reduce progressively consistent with an inversion of the groupiness after wave breaking as, on average, the highest wave before breaking is the lowest after breaking (Svendsen and Veeramony, 1977).

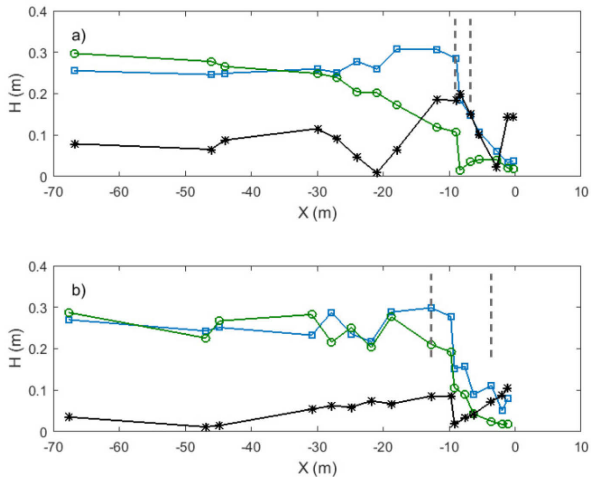

Figure 3. Cross-shore distribution for tests BE1 (a) and BE4 (b) of measured primary wave height, H_1(○) and H_2 (□) and measured wave height at f_g (∗) while wave breaking location is indicated with vertical dashed lines.

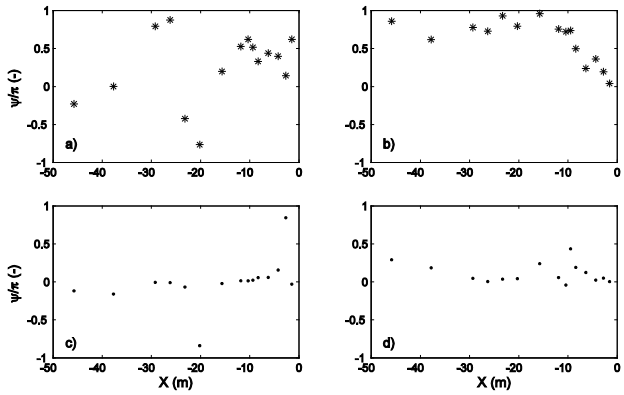

Figure 4. Phase lag ψ of *lf* waves with respect to *hf* amplitude envelope for cases (a) BE1, and (b) BE4. Phase lag ψ of *lf* waves at consecutive cross-shore locations for cases (c) BE1 and (d) BE4.

The reasons for this long wave standing pattern for case BE1 (also in BE2) but progressive for case BE4 (and BE3) is due to the radiation of long wave in a narrow surf zone area for cases BE1 and BE2. The radiated seaward long wave is in phase with the reflected long wave resulting in a large wave amplitude and standing pattern. For cases BE3 and BE4, a wider surf zone is less effective in radiating long waves and is out of phase with long wave being reflected at the shoreline. The resulting long wave pattern fro case BE4 is dominated by the incident bound long wave height. More details on the *lf* motions for these cases can be found in (Alsina et al., submitted).

3.3 *Relative contribution of short wave, long wave and mean component to the suspended sediment fluxes within the inner surf zone*

The relative influence of the difference components in the final beach evolution will depend on sediment fluxes and spatial gradients of the sediment fluxes.

Time series of horizontal velocity and sediment concentration can be decomposed into a mean and an oscillatory component. The net time averaged sediment flux (q_{net}) can be expressed as:

$$q_{net} = \langle uc \rangle = \overline{u}\,\overline{c} + \langle \tilde{u}\tilde{c} \rangle \qquad (1)$$

where the brackets indicate time averaging over the measuring time, the – overbar denotes mean component and the ~ overbar indicates oscillatory components. The oscillatory component can be also divided into high and low frequency components denoted with *hf* and *lf* sub-index respectively. Then the total net transport is expressed as:

$$q_{net} = q_m + q_{hf} + q_{lf} = \overline{u}\,\overline{c} + \langle u_{hf} c_{hf} \rangle + \langle u_{lf} c_{lf} \rangle \qquad (2)$$

where the ~overbar have been removed and cross-products between high (low) frequency velocity

components and low (high) frequency sediment concentration are considered relatively small since they are generally non-correlated.

Oscillatory sediment fluxes at different frequency components are studied using spectral techniques (Huntley and Hanes, 1987) and the cross-spectrum of velocity and concentration (*u-c*) has been computed. The integral of the *u-c* co-spectrum at the high and low frequency selected regions provides a good approximation to the time averaged sediment fluxes q_{hf} and q_{lf} in equation (2).

As the interest of this analysis is to study the relative contribution of mean and oscillatory components at the high and low frequency regions, the net sediment fluxes are also expressed as relative quantities to the total sediment mobilized in order to facilitate comparisons between different locations and to reduce variability in the transport rates between different locations or due to small variations on sensor locations relative to the bed level. We denote Q_{bulk} to the total sediment mobilized at each sensor location independently of the sign:

$$Q_{bulk} = |q_m| + |q_{hf}| + |q_{lf}| \tag{3}$$

The normalized suspended sediment fluxes (Φ_i) are then obtained as (Aagaard and Greenwood, 2008):

$$\Phi_i = \frac{q_i}{Q_{bulk}} \tag{4}$$

where the i-subindex indicates each of the sediment flux components (mean, high or low frequency), note that q_i variables denote time averaged sediment fluxes. Negative signs mean sediment fluxes seaward directed, towards the wave paddle; positive signs meaning onshoreward sediment fluxes.

The relative contribution of the different components to the suspended sediment fluxes per test case and location are showed in Table 2 in magnitudes per unit of the total (Q_{bulk}), while the cross-shore location relative to the initial shoreline and bulk suspended sediment fluxes are illustrated in Table 3. The time averaged suspended sediment flux (q_i) at each location and each component can be obtained by just multiplying the specific normalized sediment flux (Φ_i) obtained in Table 2 and the bulk magnitude (Q_{bulk}) in Table 4. For example, the *hf* time averaged sediment flux is: $q_{hf} = \Phi_{hf} \times Q_{bulk}$.

Interesting information arises from Tables 2 and 3. Firstly, at every location and for every test case, the mean current contribution to the sediment fluxes are consistently the largest contribution to the bulk sediment flux being in general about -0.7 (mean of -0.78) and negative promoting negative sediment (seaward directed) transport. The second main contribution is the wave group (*lf*) induced suspended sediment fluxes which accounts for an average of 0.18 in absolute value of the bulk sediment flux, although it shows a larger variability in magnitude and direction. Finally, the smallest contribution to the bulk sediment flux is the high frequency component accounting for an average of a 0.04 of the bulk sediment flux also with some variability in magnitude and sign, depending on sensor location and wave conditions. The three locations show many similar patterns in general, although some differences appear due to differences in the cross-shore location relative to x_0.

The high frequency component is positive most of the time at cases BE1 and BE2 but negative for cases BE3 and BE4, depending on cross-shore location relative to the initial shoreline. The reason behind this is due to the phase-lag between the incident velocity and suspended sediment peaks. In cases BE1 and BE2, the short wave component of velocity is in phase with the major suspended sediment events, onshore *hf* velocity peaks are coincident with the largest concentration peaks at the *hf* range. However, for cases BE3 and BE4, the suspended sediment concentration peaks are generally out of phase with the velocity at the *hf* components.

The *lf* influence interpretation needs to account the *lf* motions variations with the cross-shore location relative to x_0 and the long wave cross-shore structure. For BE3 and BE4, q_{lf} is predominantly negative and related to the phase lag between the *lf*-velocities and the *hf*-wave envelope.

High suspended sediment concentration (SSC) events due to larger waves within the group are close in phase to negative *lf* velocities (see also Figure 6). Whereas q_{lf} for cases BE1 and BE2 is predominantly positive due to the generally coincidence of positive *lf* velocities and larger SSC events (see also Figure 5). The phase lag between the *lf* water surface and velocity signals is due to the ingoing-outgoing influence in the velocity signal via the long wave phase velocity.

Table 2 – Contributions to the normalized suspended sediment fluxes (Φ_i) induced by mean, primary waves and wave group components.

Wave conditions	Location1 X = 71.85 m, Z = 0.05 m			Location2 X = 73.44 m, Z = 0.05 m			Location3 X = 74.82 m, Z = 0.05 m		
	Φ_m	Φ_{hf}	Φ_{lf}	Φ_m	Φ_{hf}	Φ_{lf}	Φ_m	Φ_{hf}	Φ_{lf}
BE1	-0.82	0.04	0.14	-0.71	0.09	0.20	-0.87	0.05	0.08
BE1_2	-0.78	0.05	0.17	-0.69	0.05	0.25	-0.89	0.00	-0.10
BE2	-0.88	0.02	0.10	-0.53	0.06	0.41	-0.61	0.11	0.28
BE3	-0.87	-0.05	-0.08	-0.87	-0.01	-0.11	-0.75	0.01	-0.24
BE4	-0.90	-0.04	0.07	-0.85	-0.02	-0.12	-0.81	-0.01	-0.18
BE4_2	-0.78	0.01	-0.21	-0.74	-0.06	-0.20	-0.71	-0.04	-0.25

Table 3. Total absolute suspended sediment mobilized at each sensor location, and sensor cross-shore location relative to the SWL.

Wave conditions	Location1 X = 71.85 m	Q_{bulk} (m/s)	Location 2 X = 73.44 m	Q_{bulk} (m/s)	Location3 X = 74.82 m	Q_{bulk} (m/s)
BE1	-4.13	1.685	-2.54	1.024	-1.16	0.835
BE1_2	-3.41	1.813	-1.82	1.155	-0.44	0.832
BE2	-3.76	2.406	-2.17	1.349	-0.79	0.542
BE3	-3.62	0.189	-2.03	0.213	-0.65	0.380
BE4	-3.51	0.913	-1.92	0.126	-0.54	0.113
BE4_2	-3.16	0.116	-1.57	0.120	-0.19	0.171

Wave conditions BE3 and BE4 are characterized by a long wave progressive pattern with a dominance of the ingoing long wave, as discussed in section 3.2. The long wave is out of phase with the *hf* wave groups at the breaking location but progressively the phase lag reduces in the surf zone. The long wave sediment transport is predominantly negative due to the coincidence of *lf* negative velocities and sediment suspension induced by the large waves within the group (Aagaard and Greenwood, 2008). In contrast wave conditions BE1 and BE2 are characterized by a standing long wave pattern where largest waves within the group are coincident with positive long wave velocities and large suspended sediment concentration events resulting in predominantly positive long wave induced sediment transport. Nevertheless, for all tested wave conditions and at the selected cross-shore locations the sediment transport is dominated by the mean current induced sediment transport.

3.4 *Ensemble averaged sediment transport rates*

Within the surf zone, collocated measurements of water surface elevation, flow velocity and suspended sediment concentration were available.

Figure 5 shows the ensemble average of water surface elevation, horizontal flow velocity and suspended sediment concentration at the location x =-1.86 within the surf zone for the BE1 case. Ensemble averaging has been done using the last 6 measured hydrodynamic runs for each wave conditions. This location is eroding as illustrated in Figure 2.

It is observed that the highest waves within the *hf* wave groups are in phase with the lf water surface oscillation. The reason behind this is attributed the inversion in the wave modulation after breaking (Svendsen and Veeramony, 1977, Janssen et al., 2003) but also to the standing long wave pattern within the surf zone and the outgoing influence in the filtered signal (see Figure 4a).

A strong modulation of the flow velocity at the group frequency is also observed. There is a slight phase lag between the *lf* induced water surface elevations and velocity, this phase lag is more noticeable at other locations closer to the shoreline due to the ingoing-outgoing influence in the *lf* induced velocity (Elgar and Guza, 1985) and the standing pattern discussed in the previous section. The suspended sediment concentration is highly controlled by the group frequency modulation. High waves within the group tend to be coincident with high sediment suspension events, however the highest wave does not always promote the largest suspension event and not all the wave groups promote the same sediment suspension pattern. This suggests inertial effects and time history influences on the sediment suspension response to hydrodynamics. The resultant suspended sediment flux is predominantly negative (seaward directed) due to the negative predominant velocities at the measuring location (mean return flow).

A similar plot for the BE4 case (same cross-shore location) is illustrated in Figure 6 where two wave group periods are shown for clarity. The location is also within the inner surf zone at X = -1.97 m. Case BE4 shows a larger modulation in the water surface elevation in comparison with case BE1. Wave groups are similarly in phase with the *lf* water surface elevation. In this case, the long wave water surface oscillation is not in phase with the *lf*-induced velocities due to the larger influence of ingoing long wave. The influence of individual waves in the flow velocity pattern is more noticeable than in case BE1.

Sediment suspension events appear related to individual waves forming the wave groups. However, the magnitude of the single suspended sediment events is controlled by the modulation of the water surface elevation showing higher peaks close to the crest of the *lf* signal and a modulation of the base SSC signal correlated with the *lf* water surface. Similar to condition BE1, the overall suspended sediment flux is negative due to the mean negative velocity. This location is also eroding as illustrated in Figure 2.

Interestingly the time-dependent sediment transport rate for both cases, BE1 and BE4, shows an important low frequency modulation but the positive and negative long wave sediment transport rates are of similar magnitude but with opposing direction and tend to balance each other. Thus, the mean sediment transport rate dominates.

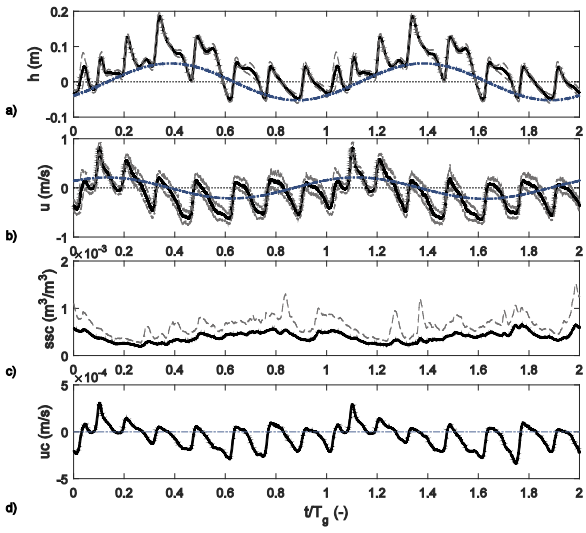

Figure 5. Ensemble average over the repetition period (T_R) of (a) water surface elevation, horizontal velocity (b) and (c) suspended sediment concentration at the location x =-1.86 m within the surf zone and wave condition BE1. Solid black lines indicate the ensemble mean values and dashed grey lines the variability over the mean using the standard deviation. Dash-dot blue lines indicate *lf* components.

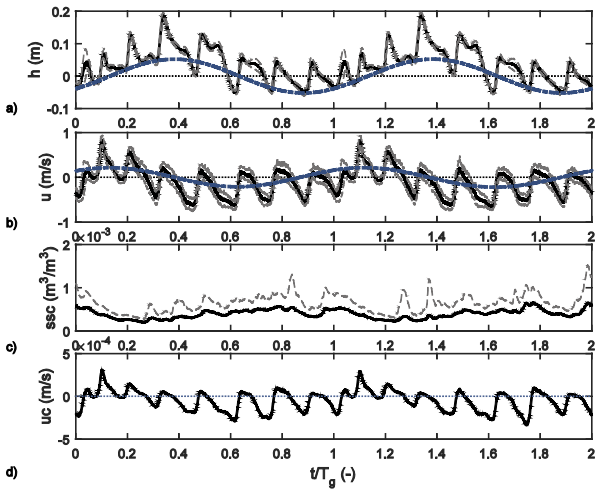

Figure 6. Ensemble average over the repetition period (T_R) of (a) water surface elevation, horizontal velocity (b) and (c) suspended sediment concentration at the location x =-1.97 m within the surf zone and wave condition BE4. Solid black lines indicate the ensemble mean values and dashed grey lines the variability over the mean using the standard deviation. Dash-dot blue lines indicate *lf* components.

4 CONCLUSION

Large-scale laboratory measurements of beach profile evolution, hydrodynamics and sediment concentration have been presented showing the influence of wave group periods in the measured beach profile morphological evolution.

Four different bichromatic conditions with similar energy content but varying the bichromatic bandwith have been tested. The measured beach profile evolution at the inner surf zone shows important differences explained from the wave group modulation. It has been shown that increasing the wave group period promotes a seaward horizontal displacement in the shoreline erosion pattern.

Moreover, the relative contribution of mean, primary waves and wave group components to the suspended sediment fluxes have been computed using spectral techniques. It has been shown that the mean component dominates the suspended sediment transport in the selected locations within the surf zone and consistently inducing negative sediment fluxes (seaward directed).

Suspended sediment fluxes computed from co-spectral analysis of velocity and SSC time series suggest a more negative tendency in the *lf*-induced sediment fluxes for narrow banded conditions (BE3 and BE4) in most locations within the inner surf zone.

Ensemble averaged time series of water surface elevation, velocity and suspended sediment concentration within the inner surf zone have shown that the *lf*-induced sediment transport is consists of a positive and negative sediment transport pattern of large magnitude but opposing signs resulting in a small net sediment transport. A net positive or negative *lf* induced sediment transport is due to asymmetries or phase lags in the *lf*-induced sediment fluxes.

The more negative tendency of the narrow bandwidth condition is explained due to the progressive nature of the long wave pattern for larger wave groups and the phase lag between the large wave crest and negative flow velocity, i.e. larger waves within the group coincident with negative velocities. The standing pattern for reduced wave group periods change the phase lag between the long wave water surface elevation and horizontal velocities.

REFERENCES

Aagaard, T. & Greenwood, B. (2008) Infragravity wave contribution to surf zone sediment transport — The role of advection. *Marine Geology,* 251**,** 1-14.

Alsina, J. M. & Cáceres, I. (2011) Sediment suspension events in the inner surf and swash zone. Measurements in large-scale and high-energy wave conditions. *Coastal Engineering,* 58**,** 657-670.

Alsina, J. M., Padilla, E. M. & Caceres, I. (submitted) Sediment transport and beach profile evolution induced by bichormatic wave groups with different group periods. *Coastal Engineering*.

Baldock, T. E., Alsina, J. A., Caceres, I., Vicinanza, D., Contestabile, P., Power, H. & Sanchez-Arcilla, A. (2011) Large-scale experiments on beach profile evolution and surf and swash zone sediment transport induced by long waves, wave groups and random waves. *Coastal Engineering,* 58**,** 214-227.

Beach, R. A. & Sternberg, R. W. (1991) Infragravity driven suspended sediment transport in the swash, inner and outer-surf zone. *Proc. Coastal Sediments'91.* ASCE.

Cáceres, I. & Alsina, J. M. (2012) A detailed, event-by-event analysis of suspended sediment concentration in the swash zone. *Continental Shelf Research,* 41**,** 61-76.

Dubarbier, B., Castelle, B., Marieu, V. & Ruessink, G. (2015) Process-based modeling of cross-shore sandbar behavior. *Coastal Engineering,* 95**,** 35-50.

Elgar, S. & Guza, R. T. (1985) Shoaling gravity waves: comparisons between field observations, linear theory, and a nonlinear model. *Journal of Fluid Mechanics,* 158**,** 47-70.

Huntley, D. A. & Hanes, D. M. (1987) Direct measurement of suspended sediment transport. *Proc. Coastal Sediments'87.* New York, A. soc. Civ. Eng. .

Janssen, T. T., Battjes, J. A. & van Dongeren, A. R. (2003) Long waves induced by short-wave groups over a sloping bottom. *Journal of Geophysical Research,* 108**,** 3252, doi:10.1029/2002JC001515, 8-1 to 8-14.

Longuet-Higgins, M. S. & Stewart, R. W. (1962) Radiation stress and mass transport in gravity waves, with application to `surf beats'. *Journal of Fluid Mechanics,* 13**,** 481-504.

Longuet-Higgins, M. S. & Stewart, R. W. (1964) Radiation stresses in water waves; a physical discussion with applications. *Deep-Sea Research,* 11**,** 529-562.

Miles, J., Butt, T. & Russell, P. (2006) Swash zone sediment dynamics: A comparison of a dissipative and an intermediate beach. *Marine Geology,* 231**,** 181-200.

Roelvink, D., Reniers, A., van Dongeren, A., van Thiel de Vries, J., McCall, R. & Lescinski, J. (2009) Modelling storm impacts on beaches, dunes and barrier islands. *Coastal Engineering,* 56**,** 1133-1152.

Ruessink, B. G., Houwman, K. T. & Hoekstra, P. (1998) The systematic contribution of transporting mechanisms to the cross-shore sediment transport in water depths of 3 to 9 m. *Marine Geology,* 152**,** 295-324.

Ruju, A., Lara, J. L. & Losada, I. J. (2014) Numerical analysis of run-up oscillations under dissipative conditions. *Coastal Engineering,* 86**,** 45-56.

Russell, P. E. (1993) Mechanisms for beach erosion during storms. *Continental Shelf Research,* 13**,** 1243-1265.

Svendsen, I. & Veeramony, J. (1977) Wave Breaking in Wave Groups. *Journal of Waterway, Port, Coastal, and Ocean Engineering,* 127**,** 200-212.

Symonds, G., Huntley, D. A. & Bowen, A. J. (1982) Two-dimensional surf beat: long wave generation by a time varying breakpoint. *Journal of Geophysical Research,* 87**,** 492-498.

van der Zanden, J., Alsina, J. M., Cáceres, I., Buijsrogge, R. H. & Ribberink, J. S. (2015) Bed level motions and sheet flow processes in the swash zone: Observations with a new conductivity-based concentration measuring technique (CCM+). *Coastal Engineering,* 105**,** 47-65.

van Dongeren, A., Battjes, J., Janssen, T., van Noorloos, J., Steenhauer, K., Steenbergen, G. & Reniers, A. (2007) Shoaling and shoreline dissipation of low-frequency waves. *Journal of Geophysical Research: Oceans,* 112**,** n/a-n/a.